



Article

A Multi-Subject Game-Based Operation Strategy for VPPs Integrating Wind-Solar-Storage

Hengyu Liu ^{1,2,*} , Qingqi Zhao ^{1,3}, Yang Liu ¹, Zuoxia Xing ¹, Dawei Hu ^{1,2}, Pengfei Zhang ¹, Zhi Zhang ²  and Jiazheng Sun ²

¹ The School of Electrical Engineering, Shenyang University of Technology, Shenyang 110870, China

² Electric Power Research Institute of State Grid Liaoning Electric Power Co., Ltd., Shenyang 110000, China

³ Skills Training Center of State Grid Liaoning Electric Power Co., Ltd., Jinzhou 121000, China

* Correspondence: lhyat@126.com; Tel.: +86-139-9823-6676

Abstract: Along with the continuous development of renewable energy sources (RES) such as wind power and photovoltaic, a large proportion of RES were connected to the power grid. However, the volatility and intermittency of RES threaten the safe and stable operation of the power system. Virtual power plants (VPPs) were introduced to solve such problems. In order to study the cooperation mode of integrating wind-solar-storage for multi VPPs, this paper established multi-objective individual and joint dispatching model for single VPP and multi VPPs with wind-solar-storage, respectively. Then, this paper analyzed the cooperation and the fair distribution of benefits between VPPs. By establishing the competitive strategies of the participating subjects and integrating the Shapley value to effectively distribute the benefits, the cooperative game theory was applied to effectively enhance the benefit in the VPP, to maximize the economic benefits, and to reduce the RES uncertainty risks and carbon emissions, which provided new ideas for the subsequent research on the optimal operation of RES and their engineering applications. NSGA-II was adopted to solve the multi-objective optimization problem. The strategy achieved a 10.1% reduction on the original peak load. It could effectively reduce the peak load of the VPP and ensure the accuracy of load regulation, to reach 12% of the total capacity of the VPP.

Keywords: virtual power plant; renewable energy source; cooperative game theory; Shapley value



Citation: Liu, H.; Zhao, Q.; Liu, Y.; Xing, Z.; Hu, D.; Zhang, P.; Zhang, Z.; Sun, J. A Multi-Subject Game-Based Operation Strategy for VPPs Integrating Wind-Solar-Storage. *Sustainability* **2023**, *15*, 6278. <https://doi.org/10.3390/su15076278>

Academic Editor: Antonio Caggiano

Received: 23 February 2023

Revised: 29 March 2023

Accepted: 31 March 2023

Published: 6 April 2023



Copyright: © 2023 by the authors. Licensee MDPI, Basel, Switzerland. This article is an open access article distributed under the terms and conditions of the Creative Commons Attribution (CC BY) license (<https://creativecommons.org/licenses/by/4.0/>).

1. Introduction

1.1. Background and Significance

At present, along with the gradual depletion of fossil fuel and the deterioration of the environment worldwide, the energy revolution attracted worldwide attention as an important part. Fossil fuels such as coal, oil and natural gas are still an important part of today's energy structure. Since the total amount of fossil energy is limited, the imbalance of its distribution and its huge demand became a problem around the world. Therefore, the continuous improvement of energy structure and the increase in power system flexibility became important means to achieve the development for low-carbon energy.

Under the strategy of “carbon peak” and “carbon neutrality”, renewable energy sources (RES), primarily wind and solar, is stochastic, intermittent and fluctuating. Meanwhile, the high proportion of RES integrated into the distribution grid has a huge impact on the grid. Virtual power plant (VPP) applies advanced communication technology to collaboratively control multiple distributed energy resources (DER) of different areas and varying types [1,2]. It integrates wind turbine (WT), photovoltaic (PV), energy storage system (ESS) and flexible load. Through rational construction and coordinated optimization, flexible dispatching of controllable power sources can smooth out the randomness and volatility of RES [3]. After achieving overall controllability of external power output, it can participate in the power market such as other power plants.

VPP realizes a new kind of power system with RES as the main source. Through advanced communication technologies and software systems, VPPs realize the aggregation and coordinated optimization of DERs [4]. VPP can participate in the power market and grid operation as a special power plant with a coordinated power management system. Thus, it is able to aggregate multiple DERs to participate in the electricity market and ancillary service market operation, solving the problems of power constraint and low energy efficiency.

1.2. Research Status

1.2.1. Status of Optimal Scheduling of VPP

It is necessary to aggregate the operating status, operating cost and operating efficiency of DERs to participate in the power market together with traditional power plants, such as thermal and hydro power plants. Therefore, VPP, the exchange of internal resources with the external grid, can sell electricity to customers and participate in electricity markets, responding to demand-side management measures such as time-of-use tariffs for external loads [5,6].

Regarding optimal scheduling within the VPP, the coordination and optimization of internal resources to maximize the operational efficiency and benefits of the VPP are the main issues. Ref. [7] extended the object of VPP aggregation to cogeneration units. Through the exchange of electricity and thermal energy in the industrial park, an optimal scheduling model of day-ahead cogeneration for VPP was established to achieve optimal scheduling of VPP. It applied mixed integer linear programming (MILP) algorithm for optimization. Ref. [8] proposed an optimal scheduling model for VPP that accounted for the synergy of electricity to gas. It could shift the waste gas energy consumption through joint scheduling to smooth out RES fluctuations, to reduce costs and carbon emissions. In [9], an array of optimization solutions were developed and applied for a community-oriented VPP aggregating renewable energy generation units. The scheduling of the VPP aims to maximize revenues and reduce penalties while addressing market constraints. In [10], a VPP solution for managing both the generation and demand sides using game theory to explore the cooperation among prosumers was presented. The profit of the VPP was allocated based on the Shapley value. In [11], an economic optimal dispatch model of VPP with peak and frequency regulation was developed. In the model, the VPP contained WT and ESS. The hybrid simulated annealing-genetic algorithm with self-adaptive parameters was adopted to cope with the non-linearity and compute the economic bidding plans for VPP.

1.2.2. Status of Demand Response in VPP

Demand response (DR), as an interactive means within the power system, effectively directs customers' electricity consumption by changing prices. It provides incentives to improve system economics and reliability [12]. VPP, as a virtual public equipment, drives demand-side and supply-side exchanges through the market. As there are multiple DERs, EES and flexible loads within VPP, VPP can be considered as a way of DR and use its characteristics to achieve the same effects as an electric power plant. In [13], the proposed VPP energy management optimization model was solved by applying the improved cooperative particle swarm optimization (ICPSO) to ensure the comfort of flexible load users. In [14], an incentive and price VPP model for DR under the condition of DR's uncertainty was established. However, it did not consider flexible loads such as air conditionings and smart refrigerators inside the DR. In [15], electric vehicles as energy storage units were established and established its VPP optimal dispatch model, using the flexibility of charging and discharging electric vehicles. It could smooth out the volatility of WT, which did not consider the superiority of joint optimal dispatch of VPP on the supply and demand sides. In [16], a VPP based on conditional value-at-risk covering DER, ESS, and flexible loads was established. Meanwhile, it designed a two-stage stochastic planning energy management model to limit the risk in a manageable range and ensure the maximization of VPP benefits.

1.2.3. Status of Game Theory in VPP

A VPP participating in electricity market bidding mainly reflects the aggregation of multiple VPPs. VPPs forms multiple DERs as a whole to participate in the competition of electricity market and trade with each other to obtain respective economic benefits [17]. In the field of optimal operation of RES, game theory is widely used in many fields such as power system planning and operation control. In the game, game parties include electricity market generating enterprises, transmission operators, industrial parks and end-users. Additionally, for enterprises, industrial parks and other larger areas, all internal subjects together form an integrated energy system, working together to maximize energy and economic benefits and to minimize carbon emissions. In [18], a two-tier VPP dispatching model was established. The upper layer was a tariff bidding model with the optimization objective of minimizing the operating cost of VPP. The lower layer was a power bidding model with the optimization objective of maximizing the economic benefits of each unit within VPP. It used Stackelberg dynamic game theory to establish a bidding dynamic game model for analysis. In [19], a VPP for electric vehicles under DR was established. It established a three-stage multi-tiring power market bidding model by considering VPP participation in day-ahead market, real-time market and bilateral contract market. The result could achieve effective control of electric vehicles and DR, reducing VPP operation cost. In [20], the relationship between VPP and DER was considered, and the study established a multi-agent system based on VPP double-layer coordination mechanism and multi-scale rolling optimization model. Between the internal VPP, DER and external multi VPPs, it used the cooperative game approach.

1.3. Main Work of the Paper

The main contributions of this paper are organized as follows.

- (1) Compared with the traditional control strategy, this paper constructs a low-carbon economy control method based on demand response (DR);
- (2) Multi-VPP cooperative game is used to optimize the internal operation cost and carbon emission of the system.

The rest of the paper is organized as follows. Section 2 establishes the VPP scheduling optimization model. The cost models of PV, WT, ESS and DR are built. On the basis, the optimal operation model for a single VPP and multi-VPP joint scheduling model are established. Section 3 describes methods for optimal solution of VPPs on the premise of the existing model in Section 2. Section 4 uses the example for two VPP models simulating to prove the effectiveness and feasibility of the proposed method. Section 5 concludes the paper.

2. VPP Scheduling Optimization Model

After determining generation demand and other information such as pre-schedule, radiation intensity, the grid dispatcher performs integrated dispatching according to the optimal dispatching model combining PV, WT and other DERs [21–23].

In this paper, it was assumed that the VPP contains a multi-energy cooperative optimization control module including WT, PV, ESS, electrical refrigeration unit (ERU), absorption refrigeration unit (ARU), utility power and other power supply. Since most users only use the single mode for energy supply, they cannot realize information sharing and multi-energy coupling. Therefore, rooftop PV, distributed WT, ESS and cold flexible load were assembled to avoid a large number of low-efficiency devices. A VPP structure diagram was obtained based on the actual area, as shown in Figure 1.

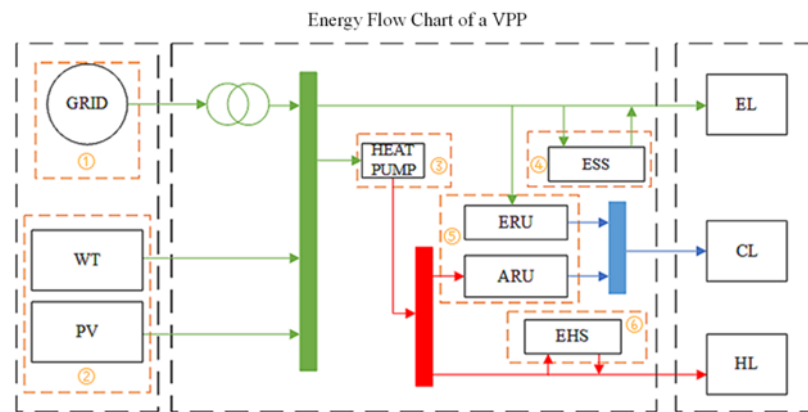


Figure 1. Structure diagram of a VPP.

Figure 1 illustrates the VPP structure in the industrial park and the directions of electricity, heat and cold flows, which are divided in three parts: generation, storage and load, including 6 kinds of equipment which are labelled in the figure. The grid with WT, PV provided the electricity to the load and other equipment. While the heat pump, ERU and ESS were active, heat and cold flows were supplied to the load. This section analyzes two optimization models for individual dispatch of a single VPP and cooperative dispatch of multiple VPPs.

2.1. Optimal Operation Model for a Single VPP

When the VPP_m was optimized separately, the cost models of PV, WT, and ESS were established. Considering DR, the VPP optimal operation model was established. The solution flow chart is shown in Figure 2. All the participating subjects were formed into a grand alliance, and the strategy was the scheduling result of each equipment. The cost that should be saved was obtained by comparing the cooperative or non-cooperative solutions in the minor alliance. Then, benefits were distributed to the major alliance after searching for feasible minor alliance solutions.

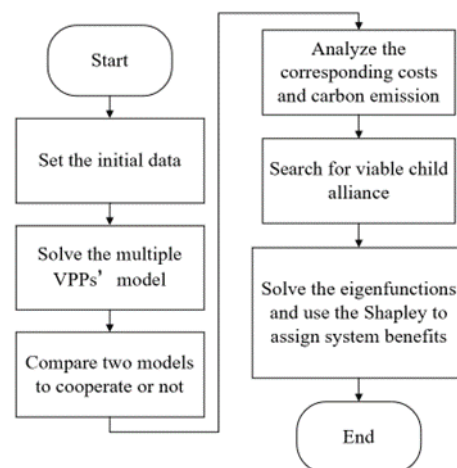


Figure 2. Flowchart of multi-subject game solving for the VPP.

The components of a single VPP can be known from the multi-subject game solution in the upper layer of the VPP. The process is to determine the cost models of PV, WT, ESS, and the cost of DR, in preparation for the subsequent establishment of the objective function of the single VPP and its constraints.

Since PV power generation is more significantly affected by weather, PV power generation is stochastic and belongs to uncontrollable DER [24]. PV power generation has a higher

power generation priority than other power generation units within the VPP. Its power generation is mainly determined by radiation. The calculation formula can be obtained as:

$$f(P_{PV}) = \frac{\Gamma(\alpha + \beta)}{P_{PV}^e \Gamma(\alpha) \Gamma(\beta)} \left(\frac{P_{PV}}{P_{PV}^e} \right)^{\alpha-1} \left(1 - \frac{P_{PV}}{P_{PV}^e} \right)^{\beta-1} \quad (1)$$

where P_{PV} is the PV power; P_{PV}^e is the rated value of PV power; α and β is the parameter of Beta distribution.

When calculating the cost of PV power generation, the electricity price differential and losses are considered. Thus, the operating cost of PV power generation can be simplified. The calculation formula can be obtained as:

$$C_{PV} = -P_{PV}^t (C_S - C_{SI}) \quad (2)$$

where P_{PV}^t is the PV power generation at the time of t ; C_S is the D-value between the PV benchmark feed-in tariff and the time-of-use tariff; C_{SI} is the operating loss cost.

To calculate the cost of wind power, the formula for WT is similar to that for PV power. Thus, the formula is as:

$$C_{wt} = -P_{wt}^t (C_w - C_{wl}) \quad (3)$$

where P_{wt}^t is the output of the wind turbine at the time of t ; C_w is the value of the wind power benchmark feed-in tariff and the time-of-use tariff; C_{wl} is the operating loss cost.

The ESS used inside the VPP is mainly a battery, which operates in two ways: charging and discharging. When there is excess power in the VPP power generation unit, the ESS charges; when the power supply in the VPP is insufficient, the ESS discharges.

To determine the unit storage power of the ESS, the amount of power is related to the efficiency and loss of charging and discharging. Thus, there is a formula as:

$$S_{bat}^t = S_{bat}^{t-1} (1 - \sigma) + \eta_{Cb} S_{Cb}^t - \frac{S_{Fb}^t}{\eta_{Fb}} \quad (4)$$

where σ is the loss rate of the ESS; S_{Cb}^t and S_{Fb}^t indicate the charging and discharging output of the ESS at the time t ; η_{Cb} and η_{Fb} indicate the charging and discharging efficiency of the ESS, respectively.

Furthermore, corresponding to the charging and discharging cost generated by the battery fully charged, the operating cost function of the ESS is obtained as shown in

$$C_{bat} = S_{Cb}^t C_{Cb} + S_{Fb}^t C_{Fb} \quad (5)$$

where it considers the depreciation cost of ESS, due to discharge depth, discharge rate and frequent charging.

To estimate the cost of external power purchase or benefit from power sales, there is an expression as:

$$C_{bs} = P_C C_g \quad (6)$$

where P_C is the magnitude of the power exchanged between the microgrid and the outside; is the time-of-use tariff at the moment.

The purpose of DR is to change the original power consumption behavior of users in the electricity market by responding to price or incentive mechanisms. DR regulates the power balance of the system by controlling cold flexible loads such as air conditionings and smart refrigerators in the VPP. Due to the economic contradiction between agency and the users of flexible loads, the compensation tariff is fixed [25,26]. As the importance of the load shedding is high, the users' compensation increases, or the agency receives less

benefit. Therefore, this paper addressed the above problem by classifying each flexible load for compensation as:

$$C_{VPP,b} = \sum_{i=0}^n S_r(i) \delta_r(i) \quad (7)$$

where $S_r(i)$ indicates the amount of load interruptions of importance i ; $\delta_r(i)$ indicates the unit compensation price of load importance i .

2.2. Multi-Objective Optimization of a Single VPP

Multi-objective optimization is used to build the internal optimization model of a single VPP with application of internal components and the flexible load. The objective function was established with maximization of economic benefits and minimization of carbon emissions.

(1) Economic objectives

The economic objective was to ensure the lowest cost of system operation optimization, which is indicated by

$$\min F = C_{bs} + \sum_{t=1}^{24} C_{PV} \varphi_{PV}^t + C_{bat} \varphi_{bat}^t + C_{wt} \varphi_{wt}^t + C_{VPP,b} \varphi_{vpp}^t \quad (8)$$

where F is the total operational cost of the system; φ_{PV}^t denotes the PV operating state at time t , with a value of 0 or 1; φ_{bat}^t denotes the ESS operating state at time t , with a value of 0 or 1; φ_{wt}^t denotes the WT operating state at time t , with a value of 0 or 1; φ_{vpp}^t denotes the interruption of the flexible load at time t with a value of 0 or 1. The formula is the cumulative minimum value of each cost of the virtual plant at 24 h of the day.

(2) Environmental objectives

The environmental objective is to ensure that the emissions of pollutants is minimized, as expressed by

$$\min P_{to} = \sum_{t=1}^T [P_C \mu_C + S_{Db} \eta \mu_b] \quad (9)$$

where μ_C and μ_b are the CO₂ emission factors of grid connection power and ESS output power, respectively; η is the power exchange factor.

A VPP is equivalent to a multi-energy coordinated system. In order to ensure the stability of energy consumption and minimize the cost, the system needs to achieve a balance between supply and demand for cooling, heating and electrical loads. Meanwhile, various energy supply devices in the system must meet their own operational constraints during operation. All above constitute the constraints of the system operation. The constraints are as follows.

(1) Constraint on power limit in interconnecting line

$$|P_C| \leq P_{\max} \quad (10)$$

where P_C is the magnitude of power exchanged between microgrid and main grid; P_{\max} is the limit of power exchanged between microgrid and main grid.

(2) Constraint on the charge and discharge limits of the battery

$$0 \leq P_{Db} \leq P_{Db,\max}, P_{Cb,\max} \leq P_{Cb} \leq 0 \quad (11)$$

where $P_{Db}, P_{Db,\max}$ are the discharge power and maximum discharge power of the ESS; $P_{Cb}, P_{Cb,\max}$ are the charging power and maximum charging power of the ESS.

(3) Constraint on the SOC

$$SOC_{\min} \leq SOC \leq SOC_{\max} \quad (12)$$

where SOC is the state of charge of the energy storage battery, SOC_{min} , SOC_{max} are the upper and lower limits of the allowable power during the operation of the ESS.

- (4) Constraint on the upper and lower limits of PV and WT's output

$$\begin{aligned} P_{s,min} &\leq P_s \leq P_{s,max} \\ P_{w,min} &\leq P_w \leq P_{w,max} \end{aligned} \quad (13)$$

where $P_{s,min}$, $P_{s,max}$ are the maximum active power output and minimum active power output of PV in MPPT mode; $P_{w,min}$, $P_{w,max}$ are the maximum active power output and minimum active power output of the WT.

- (5) Constraints on interruptible load interruption

$$\varphi_{vpp}^t S_{r,min} \leq \sum_{i=0}^n S_r(i) \leq \varphi_{vpp}^t S_{r,max} \quad (14)$$

2.3. Multi-VPP Joint Scheduling Model

Based on the multi-objective optimization of a single VPP, a cooperative game model with multi VPPs was constructed in the cooperative mode. To maximize the profit of each VPP, the internal members of each VPP was regulated responding to the operational requirements. Multiple VPPs participate in the market competition as market players in the electricity market. Each of them improved its own benefit, ensuring the safe and economic operation of the grid. Therefore, this section adopted the cooperative game approach of multiple VPPs.

Suppose that the VPP_a is optimized individually with the number of scenarios S_a ; the probability of scenario s is γ_a^s ; the scheduling duration is Δt ; the total time is T ; the total number of power supplies N ; the power supply n corresponds to the power output benefit C_a^n .

The main source of benefit for VPP is related to the benefit from the actual output of the DERs and the cost of VPP due to output deviations. Thus, there is the maximum benefit for a single VPP optimization.

$$C_{VPP}^a = \max \sum_{s=1}^{S_a} \gamma_a^s \sum_{t=1}^T \left[\sum_{n=1}^N C_a^n \cdot S_{nt}^{as} - c^+ F(\Delta S_t^{as}) - c^- F(-\Delta S_t^{as}) \right] \Delta t \quad (15)$$

where c^+ and c^- indicate the upward and downward standby prices of the power plant; S_{nt}^{as} is the output of power supply n at time t under scenario s for VPP_a; ΔS_t^{as} is the difference between the planned and actual output; $F(x)$ is the segmentation function, as follows.

$$F(x) = \begin{cases} x & x > 0 \\ 0 & x \leq 0 \end{cases} \quad (16)$$

Further for multi-VPP co-optimization, it assumes M VPPs form an alliance B. Therefore, there is a maximum benefit of VPP alliance B.

$$C_{VPP}^{co} = \max \sum_{s=1}^{S_a} \gamma_b^s \sum_{t=1}^T \left[\sum_{m=1}^M \sum_{n=1}^N C_m^n \cdot S_{nt}^{ms} - c^+ F(\Delta S_t^{hs}) - c^- F(-\Delta S_t^{hs}) \right] \Delta t \quad (17)$$

where C_m^n is the power output benefit corresponding to plant m ; S_{nt}^{ms} is the output of the VPP_m at scenario s for power supply n at the time of t ; ΔS_t^{hs} is the difference between the planned and actual output of the alliance.

Eventually, M VPPs V_1, V_2, \dots, V_m can form alliances such as $\{V_1\}, \{V_1, V_2, \dots, V_m\}$. Thus, there are alliance characteristic functions as

$$\begin{aligned} v(\{V_m\}) &= 0 \\ v(\{V_1, V_2, \dots, V_m\}) &= c(\{V_1, V_2, \dots, V_m\}) - \sum_{x \in \{V_1, V_2, \dots, V_m\}} c(x) \end{aligned} \quad (18)$$

where $c(\{V_1, V_2, \dots, V_m\})$ indicates the benefit when m VPP alliances are run optimally; $c(x)$ indicates the benefit when x is taken as V_m in $c(x)$ for m separate runs of the VPP.

Alternatively, the individual rationality and the group rationality of the cooperative game are determined simultaneously.

(1) group rationality:

$$x_{V_1} + x_{V_2} + \dots + x_{V_M} = v(\{V_1, V_2, \dots, V_M\}) \quad (19)$$

(2) individual rationality:

$$x_{V_m} \geq v(\{V_m\}) \quad (20)$$

3. Methods for Optimal Solution of VPPs

3.1. Multi-Objective Optimization

3.1.1. NSGA-II

Non-dominated sorting genetic algorithm II (NSGA-II) is an evolutionary algorithm used to analyze and solve multi-objective optimization problems. Based on the fitness of each solution within the population, it applies a fast non-dominated ranking algorithm to stratify the current population of individuals. In the same layer, there is no dominance relationship among the individuals. Then, to enrich the population diversity, crowding distance is used to measure the density of individuals near the solved solution. In turn, the superiority of individuals within the same layer is judged [27–29]. Finally, an elite sampling strategy for parent–child mixed is developed to reduce the loss rate of good individuals from the previous generation of the population. It improves the evolutionary speed of the population and enhances the algorithm timeliness.

Figure 3 indicates the NSGA-II algorithm flowchart, which is divided into three main parts. The first part is the initial definition. Firstly, the population is initialized. The number of objective functions and the population size are determined. Additionally, non-dominated sorting is then performed to determine the number of dominated individuals and the set of dominated solutions of known individuals. The diversity of individuals in the population is preserved by selection, crossover and variation. The second part is the elite selection. The number of new populations after the parent–child merger is determined. Then, the screened individuals are sorted quickly in non-dominated. They are screened according to the calculated crowding. The third part is the iteration, where the offspring are selected, crossed and mutated until the number of iterations is reached.

3.1.2. Model Solving Process

The whole optimized solution is shown in Figure 4. The optimal result was obtained by updating and sorting the population, and then, the cooperative game problem of multiple VPPs was solved.

1. Input data. The operating cost of DERs in a VPP is calculated to obtain the total system operating cost;
2. Randomly generate the initial population. Based on the economic and environmental objectives, it calculates the individual objective function values that satisfy the power supply constraints;
3. Fast non-dominated sorting of the initial population. It gets good sires based on individual stratification and crowding information to obtain offspring populations;

4. Based on power and output constraints, the elite strategy was applied to select, crossover and mutate. Then, preserve the diversity of individuals in the population and select a new generation of same-sized parents;
5. Determine if the maximum number of iterations is reached. if so, exit the calculation. Otherwise, go back to step (3) and continue;
6. Input the optimized values into the calculation of VPP after iteration to the upper limit, to solve the cooperative game constraints of multi-VPPs. Then, output the operational optimized values of each VPP after the solution satisfies each benefit constraint.

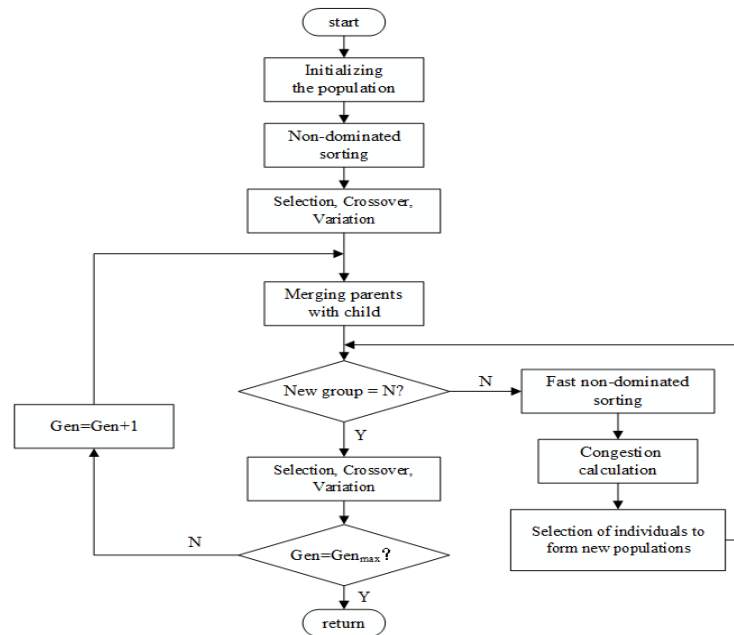


Figure 3. Flowchart of NSGA-II optimization algorithm.

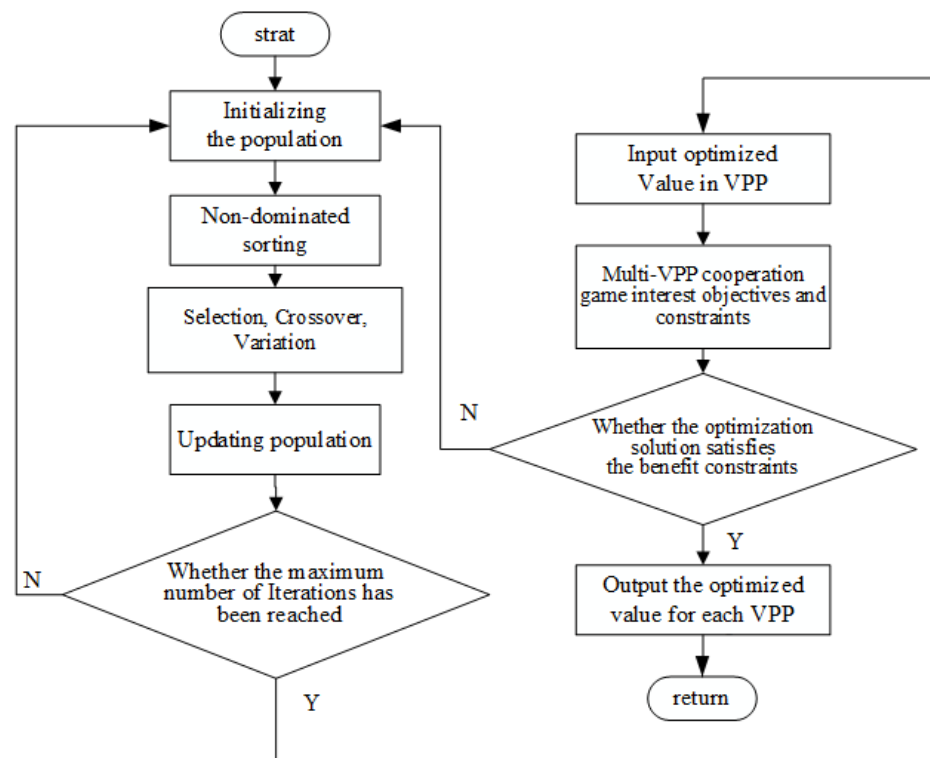


Figure 4. Flowchart of optimized solution.

3.2. Cooperative Game

A cooperative game is a game in which participants can jointly reach a binding and enforceable agreement [30]. Its objectives are mainly alliance formation and game distribution. The key to the cooperative game is how participants form an alliance and how to redistribute the alliance payments. Since participants in the alliance are different VPPs composed of WT, PV and ESS, the marginal benefits per unit of ESS are different. After determining the multi-VPP objective function and constraints in Section 2.3, it will establish the cooperative game model.

1. Participants: VPP_a contains N_1 WTs and N_2 PVs internally, in which any n_i WTs and n_j PVs can constitute an alliance A of VPPs. Meanwhile, there are N ESSs and M VPPs externally, of which m VPP grand alliance B ;
2. Strategy set: the actual power exchange with the shared energy storage for each participant of alliance A at each time slot is $P_{i,t}$. The alliance B power exchange is ΔS_{nt}^{as} ;
3. Characteristic function: alliance A maximizes the VPP benefit C_{VPP}^a decided by the actual power exchange $P_{i,t}$ of each participant, who shared energy storage at each time slot. The max benefit can be indicated as $\max C_{VPP}^a$. While for alliance B , there is $\max C_{VPP}^o$. Each participant can decide how to make an alliance by comparing its own benefits under different stable alliance structures.

3.3. Distribution of Benefits

In an alliance formed by a multi-VPP cooperative game, the system reduces bidding deviations and penalties to increase the total benefit through the usefulness coordination of each VPP [31]. How to distribute the benefits among VPPs is directly related to the achievement of multi-VPP cooperation. Therefore, according to the cooperative game model constructed in this paper, the analysis of certain participants in the alliance leave the grand alliance to form a new sub-consortium. When two sub-alliances optimize the operation of their respective systems, the inability of close coupling between equipment will inevitably lead to waste or shortage of resources. The cost of the system's energy supply will also increase fast.

$$\begin{aligned}
 V(S_1 \cup S_2) &= \min_{\xi \in S^*(S_1 \cup S_2)} \max_{\eta \in S^*(I - \{S_1 \cup S_2\})} U(\xi, \eta) \leq \\
 &\min_{\xi \in S^*(S_1 \cup S_2)} \left\{ \max_{\eta \in S^*(I - S_1)} U(\xi, \eta) + \max_{\eta \in S^*(I - S_2)} U(\xi, \eta) \right\} \leq \\
 &\left\{ \min_{\xi \in S^*(S_1)} \max_{\eta \in S^*(I - S_1)} U(\xi, \eta) + \min_{\xi \in S^*(S_2)} \max_{\eta \in S^*(I - S_2)} U(\xi, \eta) \right\} = \\
 &V(S_1) + V(S_2)
 \end{aligned} \tag{21}$$

Simultaneously, it can be determined that the eigenfunctions of the cooperative game model constructed in this paper satisfy the following conditions.

$$V(S_1 \cup S_2) \leq V(S_1) + V(S_2), S_1 \cap S_2 = \emptyset \tag{22}$$

Cooperative game theory deals with the problem of multi-participant cooperation to reach the maximum benefit of the alliance and the distribution of the benefit. The Shapley method is a method of distributing the benefit according to the contribution made by individuals to the alliance. The key is to distribute equitably according to the degree of contribution of n members to the goal of the alliance. The more they contribute, the more the benefit they have [32]. In this section, the Shapley value method was used to study the multi-VPP benefit distribution problem.

$$\varphi_i(v) = \sum_{i \in S} \omega(|S_i|) \cdot [v(S) - v(S - \{i\})] \tag{23}$$

$$\omega(|S_i|) = \frac{(|S_i| - 1)!(n - |S_i|)!}{n!} \quad (24)$$

where $\varphi_i(v)$ is the benefit received by the i th member of the alliance; $|S_i|$ is the number of participants in the alliance; $\omega(|S_i|)$ is the weighting factor of the i th member; n is the number of members in the cooperative game system of the VPPs; $n!$ is the number of all possible permutations of the participants in all cooperative games; $v(S)$ is the operating benefit of the overall alliance of VPPs; $v(S - \{i\})$ is the operating benefit of the cooperative alliance after the alliance S removes i .

From the Shapley value, the multi-dimensional contribution of the participating subjects in the alliance is considered. The subjects with more multi-dimensional contribution are given more benefits as an incentive. The benefits are then allocated to the integrated economics and carbon emissions of ESS, thermal storage devices, rooftop PV and distributed WT within the VPP. In turn, the low carbon operation control strategy formed will be considered into the VPP to participate in electricity market.

4. Example Analysis

4.1. Parameters of the Algorithm

In this section, a regional VPP was used as an arithmetic example for analysis. The VPP includes one PV plant named PV1 and one WT named W1 inside, whose rated power generation was 7 MW and 2 MW. All the power of actual generation and planning were derived from the actual site data, as shown in Table 1.

Table 1. Constants of the regional VPP.

Constants of the VPP		Data
SOC_{max} / SOC_{min}	The upper/lower limit of the charge state of the ESS	1/0.4
$P_{ESS}^{ch} / P_{ESS}^{dch}$	The charging/discharging power of the ESS	5 MW/5 MW
$P_{max}^{grid} / P_{min}^{grid}$	The upper/lower limit of exchange power between microgrid	30 MW/20 MW
$p_{peak}^{grid} / p_{flat}^{grid} / p_{valley}^{grid}$	The prices of peak/flat/valley in the microgrid exchange	1.230 CNY/(kW·h)/ 0.820 CNY/(kW·h)/ 0.410 CNY/(kW·h); 1.384 CNY/(kW·h)/
$p_{peak}^{PV} / p_{flat}^{PV} / p_{valley}^{PV}$	The prices of peak/flat/valley in PV	0.923 CNY/(kW·h)/ 0.461 CNY/(kW·h); 2.153 CNY/(kW·h)/
$p_{peak}^{WT} / p_{flat}^{WT} / p_{valley}^{WT}$	The prices of peak, flat, valley in WT	1.436 CNY/(kW·h)/ 0.718 CNY/(kW·h);
The operating loss cost	_____	0.166/(kW·h)
depreciation life of ESS	_____	10 years
depreciation costs of ESS	_____	866 CNY

4.2. Simulations

This section conducts simulation analysis based on the cooperative game model and benefit distribution method above. Then, the validity of the model is verified by comparing the operation under different decision variables.

4.2.1. Single VPP Operation Optimization

Based on the models in Sections 2.2 and 2.3, the NSGA-II algorithm was used to solve the multi-VPP cooperative game model. It set the population size to 400 and the number of iterations to 50. The Pareto optimal solution set obtained from the solution is shown in Figure 5.

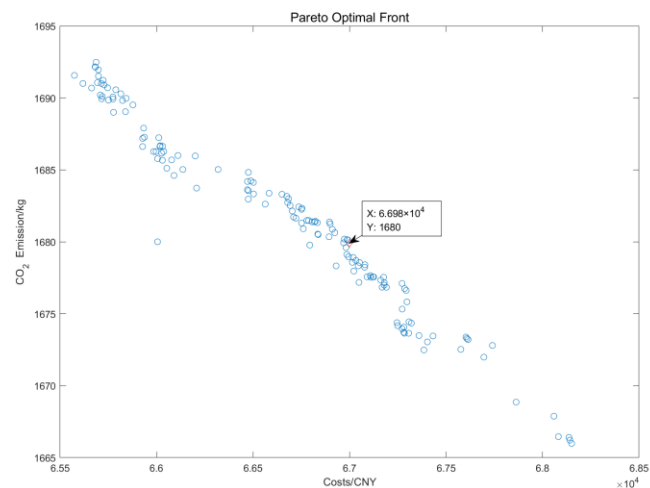


Figure 5. $\{V_1\}$ Pareto-optimal solution set.

From Figure 5, it can be concluded that the lowest cost and the lowest CO₂ emissions were mutually exclusive objectives. The reduction in one side must be accompanied by the increase in the other side. Therefore, this paper used the TOPSIS method [33–35] to find the relative optimal solution, as shown in the marked points in Figure 5.

From Figure 6, the optimized power curve was obtained. From the curve above, it can be found that the net profit of each VPP in five periods, 23:00–0:00, 0:00–1:00, 1:00–2:00, 2:00–3:00 and 3:00–4:00, was less than that of other periods, while in three periods of 11:00–12:00, 12:00–13:00 and 19:00–20:00, the net profit of each VPP was more than that of other periods. ESS was mainly charged from 10:00 to 17:00 and discharged from 6:00 to 9:00 and 18:00 to 22:00, to maintain the normal operation of the VPP.

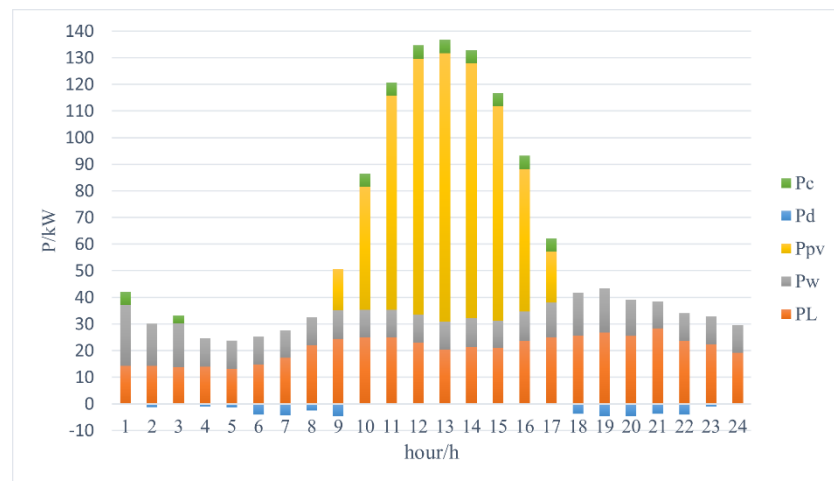


Figure 6. Optimized 24 h power curve.

It can be seen from Figure 7 that after changing PV capacity, ESS discharged to maintain the normal operation of the system in the period of 3:00–21:00. In the period of 0:00–1:00 and 1:00–2:00, ESS charges and VPP shaves peaked and filled valleys. It controlled the load control accuracy and capacity in the park.

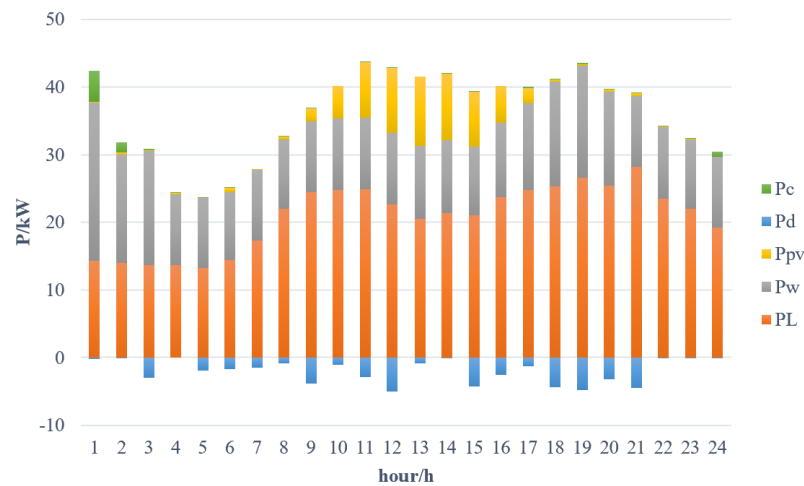


Figure 7. Optimized 24 h power curve with small PV capacity.

In addition, for the independent operation of each subject in the VPP, the respective operating results were obtained as shown in Table 2.

Table 2. Results of the Operation of Each Subject of the Independent VPP.

Subjects	Cost/($\times 10^4$ CNY)	Carbon Emissions/($\times 10^3$ kg)
Grid	2.532	0.860
ESS	1.421	0.661
PV	1.145	0
WT	0.922	0

The subjects of the single VPP in the table were the microgrid exchange power (grid), the charging and discharging power of EES (EES), the PV power (PV) and the WT power (WT). Within the single VPP, the ESS was charged during the valley period and discharged during the peak period, fully enjoying the peak-valley price difference. and the system prioritized the consumption of renewable energy, so that the optimal dispatching scheme can be derived in the sub-alliance $\{V_1\}$ of the independent VPP based on the strategy and energy price.

4.2.2. Multi-VPP Operation Optimization

In this section, three types of VPPs were used for cooperative games. Firstly, the total cost and the respective cost of the alliance were determined by the Pareto front. Additionally, it formed sub alliances of VPP $\{V_1\}$, $\{V_2\}$, $\{V_3\}$ with ESS, PV and WT. Finally, by establishing the alliance $\{\{V_1\}, \{V_2\}\}$, $\{\{V_1\}, \{V_3\}\}$, $\{\{V_2\}, \{V_3\}\}$, $\{\{V_1\}, \{V_2\}, \{V_3\}\}$, three VPPs were computed and the sub-leagues are shown in Table 3.

Table 3. Internal structure of each sub-league.

Sub-League	Microgrid Exchange	ESS	PV	WT
$\{V_1\}$	YES	Medium	1	1
$\{V_2\}$	YES	Large	3	2
$\{V_3\}$	YES	Small	0	1

Since the benefit of the alliance mainly comes from WT and PV, the total benefit of the alliance is shown in the following formula.

$$\sum_{i=1}^3 \sum_{t=1}^{24} (K_i P_{PV}^t c_{PV} + L_i P_{wt}^t c_{wt}) \quad (25)$$

where K_i , L_i are the number of PVs and WTs of the i th virtual power plant in the alliance; c_{PV}, c_{WT} are indicated as PV benefit of 0.391 CNY/(kW·h) and WT benefit of 0.48 CNY/(kW·h), respectively.

Through the calculation, the intra-alliance PV benefit of 9780.16 CNY, total WT benefit of 12,006.34 CNY, and total benefit of 21,786.5 CNY were obtained. Then, for each VPP, $\{V_1\}$, $\{V_2\}$ and $\{V_3\}$ formed an alliance for optimization. The respective marginal contribution rates of the sub-alliance $\{V_1, V_2, V_3\}$ were obtained by the cost within 24 h of the big alliance. The big alliance was synthesized by each sub-alliance and so, the total benefit was allocated. Figure 8 shows the Pareto front and the optimal solution for the total cost-carbon emission of $\{V_1, V_2, V_3\}$ alliance.

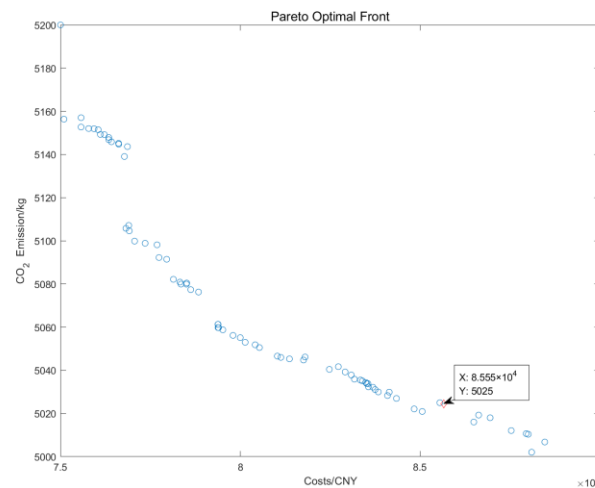


Figure 8. $\{V_1, V_2, V_3\}$ Pareto optimal solution set.

The total cost of the alliance and the total carbon emissions are shown in Figure 8. The overall output of the VPP was more consistent with the load curve when cooperating. It played a role in peak shaving and valley filling. However, since loads in the VPP takes on the peak-shaving and valley-filling work in the cooperation [36], it reduces the ability to act standby in the grid. The standby cost of the VPP increased, which needs to be reallocated for the cooperation benefits.

From Figure 9, the multi-VPP optimized power curve was obtained. From the curve above, it was found that the power of $\{V_1\}$, $\{V_2\}$ and $\{V_3\}$ were shown. The net profit of each VPP in five periods, 22:00–23:00, 23:00–0:00, 4:00–5:00, 5:00–6:00 and 7:00–8:00, was less than that of other periods, while in four periods of 11:00–12:00, 12:00–13:00, 13:00–14:00 and 16:00–17:00, the net profit of each VPP was more than that of other periods. ESS was mainly charged from 9:00 to 17:00 and discharged from 6:00 to 9:00 and 18:00 to 23:00, to maintain the normal operation of the alliance.

Meanwhile, the improved load curve obtained from the load power curve was compared with the original load curve, as shown in Figure 10. From Figure 10, it was seen that the DR-oriented VPP could effectively shave the peak. The peak of the original load curve was 60.278 MW, while the peak of the VPP was 54.019 MW after shaving the peak and filling the valley. It achieved 10.1% of the peak load of the VPP, and the accuracy of load regulation in the VPP reached 12% of the total capacity of the VPP.

As a result, through the benefit distribution of each sub-alliance, it can be concluded that the multi-VPP system constructed based on the cooperative game was involved in the economic operation of the power grid and low-carbon economic operation. It was well suited to reduce the peak load of the VPP and could ensure the accuracy of load regulation within the VPP up to 12% of the total capacity of the VPP.

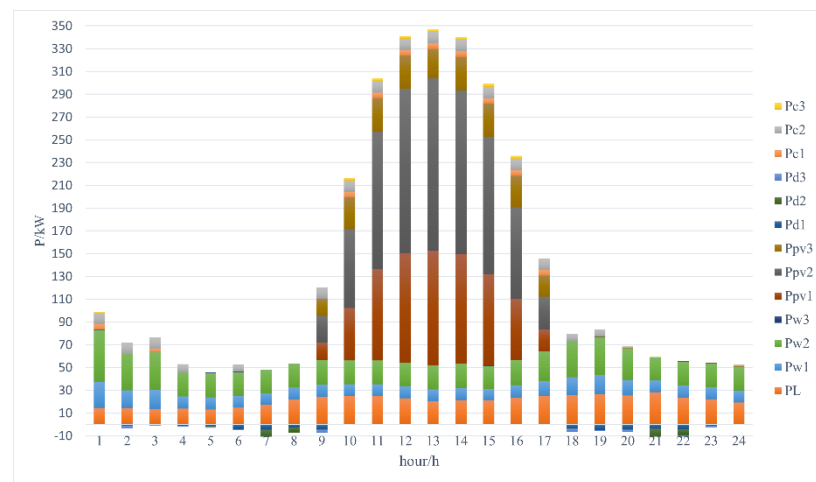


Figure 9. Multi-VPP optimized 24 h power curve.

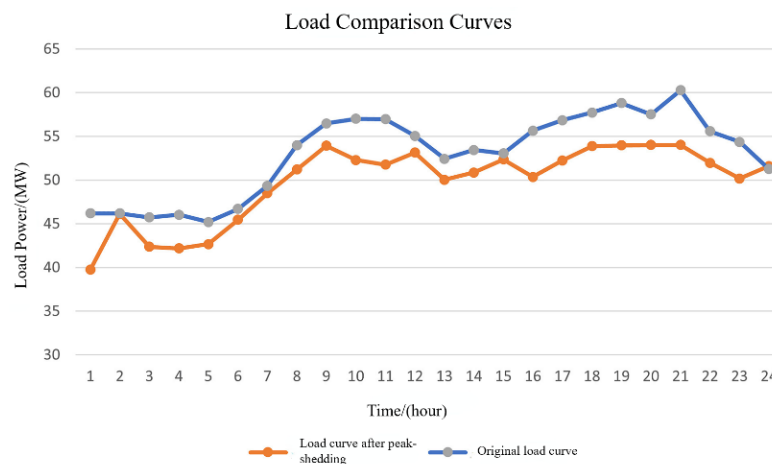


Figure 10. Load comparison curves.

4.3. Distribution of Cooperation Benefit

From Sections 3.3 and 4.2, it can be seen that the benefit of a single VPP $\{V_1\}$ of 5446.62 CNY was allocated to the benefits using the Shapley value. It requires consideration of the marginal contribution of the subject to all the sub-alliances in which it participates. For sub-alliances, the analysis was as follows.

1. The subject of the ESS can obtain the benefits from the difference between peak and valley electricity prices. At the same time, since it can improve the RES consumption as well as system stability and reduce carbon emissions, it obtains higher benefits than the direct distribution [37].
2. The direct benefit distribution of the grid was 1158.9 CNY. Since the economics of power purchase by the grid was low, and loads in the peak period coincided with the price, the benefit distribution was 10,835 CNY, according to the Shapley value of economics. However, most carbon emissions of the electricity, which was purchased from the grid, needed to be borne by the power plant. The power purchaser only bore a small portion of the carbon emissions. Therefore, a small reduction in CO₂ emissions can be achieved. Under the comprehensive analysis, the benefit distribution of the grid was 11,247 CNY.
3. The direct benefit distribution and the economic Shapley value were both 1077.3 CNY for the renewable energy mains, because of its high economics and the unchangeable power output. Meanwhile, since it had good carbon reduction effect, the final comprehensive benefit distribution was 1083.5 CNY.

After the benefit distribution, the benefits of the sub-alliance $\{V_1\}$ were obtained. Further, the cooperative game of each VPP sub-alliance is shown in Table 3. After the cooperative scheduling by Shapley value, the total benefit distribution value of each sub-alliance was obtained.

When there was only one participant in each different alliance, i.e., the alliance is $\{\{V_1\}, \{V_2\}, \{V_3\}\}$, the VPP alliance degenerated into a situation where the three were independent of each other. Its benefit considered the single VPPs' power sales benefit, the respective benefit of error reduction penalty and the benefit for wind and light abandonment penalty reduction. The total benefit for the three VPPs was 2.1786×10^5 CNY. Taking VPP1 as an example, there are three ways for VPP1 to participate in the alliance, namely $\{\{V_1, V_2\}, \{V_3\}\}$, $\{\{V_1, V_3\}, \{V_2\}\}$ and $\{V_1, V_2, V_3\}$. VPP1 decides how to alliance according to its own benefit in different alliance methods. The results of total alliance benefit and carbon emission under different alliance are shown in Table 4. From Table 4, when the alliance was $\{V_1, V_2, V_3\}$, all subjects in the alliance were optimally dispatched in cooperation. At this time, the total alliance benefit was the highest, 2.3526×10^5 CNY. Meanwhile, the carbon emissions were the lowest, so the cooperative alliance of $\{V_1, V_2, V_3\}$ would be chosen.

Table 4. Total Alliance Benefits and Carbon Emissions under Different Alliance Approaches.

NO.	Alliance Method	Total Alliance Benefit ($\times 10^5$ CNY)	Carbon Emissions (kg)
1	$\{\{V_1\}, \{V_2\}, \{V_3\}\}$	2.1786	5025
2	$\{\{V_1, V_2\}, \{V_3\}\}$	2.2476	5012
3	$\{\{V_1, V_3\}, \{V_2\}\}$	2.3380	5015
4	$\{V_1, V_2, V_3\}$	2.3526	5004

Additionally, the large alliance $\{V_1, V_2, V_3\}$ will receive the benefit of 23,526 CNY, according to the Shapley. It receives the respective benefit as shown in Table 5.

Table 5. Sub-leagues $\{V_1\}, \{V_2\}, \{V_3\}$ Benefits Distribution.

NO.	Sub-League	Benefit/ $(\times 10^5$ CNY)
1	$\{V_1\}$	0.7058
2	$\{V_2\}$	1.1763
3	$\{V_3\}$	0.4705

5. Conclusions

In this paper, a cooperative game model, considering economics and carbon emissions, was constructed for a cooperative VPP alliance formed by different VPPs. The NSGA-II optimization algorithm was applied to solve the model. The benefits of the alliance were allocated using the Shapley value, based on economics and carbon emission reduction. The results of the study show that:

1. The sub-alliance was constructed by different subjects within the single VPP. Through cooperation, it can effectively improve the energy utilization efficiency and reduce the operation cost and CO₂ emission in the system.
2. This paper applied the NSGA-II optimization algorithm to solve the cost-carbon emission function of the alliance. It will have high operational efficiency and the ability of optimal finding.
3. The Shapley value proposed in this paper, which considered the economics and carbon emission reduction, could more reasonably allocate the benefits of each subject in the system. It can motivate more single VPPs to participate in the formation of cooperative VPP alliances.
4. The data showed that the peak load of the VPP was 54.019 MW, which reduced 10.1% of the original peak load. It was better suited to reduce the peak load of the VPP and could ensure the accuracy of load regulation in the VPP to reach 12% of the total

capacity of the VPP. Meanwhile, the multi-VPP system based on cooperative game could better achieve the maximum benefit and minimum carbon emission.

Author Contributions: Conceptualization, H.L.; Methodology, Q.Z. and Y.L.; Software, Z.X.; Validation, Y.L., Z.X., D.H. and J.S.; Formal analysis, H.L. and Z.Z.; Investigation, Q.Z. and P.Z.; Data curation, D.H.; Writing—original draft, H.L. and Q.Z. All authors have read and agreed to the published version of the manuscript.

Funding: This research received no external funding.

Conflicts of Interest: The authors declare no conflict of interest.

References

1. Tian, L.; Cheng, L.; Guo, J.; Wang, X.; Yun, Q.; Gao, W. A Review on the Study of Management and Interaction Mechanism for Distributed Energy in Virtual Power Plants. *Dianwang Jishu/Power Syst. Technol.* **2020**, *44*, 2097–2108.
2. Bai, X.; Fan, Y.; Wang, T.; Liu, Y.; Nie, X.; Yan, C. Dynamic aggregation method of virtual power plants considering reliability of renewable energy. *Dianli Zidonghua Shebei/Electr. Power Autom. Equip.* **2022**, *42*, 102–110.
3. Lu, Y.; Yang, M.; Yin, S.; Chen, X.; Gu, X.; Jin, M.; Chai, Z.; Guo, X. Research on self-balancing transaction scheduling strategy of new energy power in County considering section load rate. In Proceedings of the E3S Web of Conferences, Shenyang, China, 24–25 September 2022; volume 358.
4. Han, Y.; Wang, W.; Yu, T.; Huang, Y.; Liu, D.; Jia, H. Analysis of Economic Operation Model for Virtual Power Plants Considering the Uncertainties of Renewable Energy Power Generation. In Proceedings of the 2021 IEEE Sustainable Power and Energy Conference (iSPEC), Nanjing, China, 25–27 November 2021.
5. Swantje, S.; Katrin, R.; Jürgen, M. Consumers' Willingness to Accept Time-of-Use Tariffs for Shifting Electricity Demand. *Energies* **2020**, *13*, 1895.
6. Yi, Z.; Xu, Y.; Wu, W. Market Clearing Strategy for Distribution System Considering Multiple Power Commodities Offered by Virtual Power Plant. *Dianli Xitong Zidonghua/Autom. Electr. Power Syst.* **2020**, *44*, 143–151.
7. Dehghanniri, M.F.; Golkar, M.A.; Olanlari, F.G. Power exchanging of a VPP with its neighboring VPPs and participating in Day-ahead and spinning reserve markets. In Proceedings of the 2022 30th International Conference on Electrical Engineering (ICEE), Tehran, Iran, 17–19 May 2022.
8. Wu, Y.; Wu, J.; De, G.; Fan, W. Research on Optimal Operation Model of Virtual Electric Power Plant Considering Net-Zero Carbon Emission. *Sustainability* **2022**, *14*, 3276. [[CrossRef](#)]
9. Elgamal, A.H.; Kocher-Oberlehner, G.; Robu, V.; Andoni, M. Optimization of a multiple-scale renewable energy-based virtual power plant in the UK. *Appl. Energy* **2019**, *256*, 306–322. [[CrossRef](#)]
10. Wang, Y.; Gao, W.; Qian, F.; Li, Y. Evaluation of economic benefits of virtual power plant between demand and plant sides based on cooperative game theory. *Energy Convers. Manag.* **2021**, *238*, 114180. [[CrossRef](#)]
11. Zhongkai, Y.; Yinliang, X.; Hongbin, S. Self-adaptive hybrid algorithm based bi-level approach for virtual power plant bidding in multiple retail markets. *IET Gener. Transm. Distrib.* **2020**, *14*, 3762–3773.
12. Zhou, B.; Xia, J.; Yang, D.; Li, G.; Xiao, J.; Cao, J.; Bu, S.; Littler, T. Multi-time scale optimal scheduling model for active distribution grid with desalination loads considering uncertainty of demand response. *Desalination* **2021**, *517*, 115262. [[CrossRef](#)]
13. Yu, D.; Zhao, X.; Wang, Y.; Jiang, L.; Liu, H. Research on Energy Management of a Virtual Power Plant Based on the Improved Cooperative Particle Swarm Optimization Algorithm. *Front. Energy Res.* **2022**, *10*, 21. [[CrossRef](#)]
14. Zamani, A.G.; Zakariazadeh, A.; Jadid, S. Day-ahead resource scheduling of a renewable energy based virtual power plant. *Appl. Energy* **2016**, *169*, 324–340. [[CrossRef](#)]
15. Nakamura, Y.; Omori, H. A Local VPP with EVs in Very Small Areas. In Proceedings of the 2022 International Power Electronics Conference (IPEC-Himeji 2022-ECCE Asia), Himeji, Japan, 15–19 May 2022.
16. Dabbagh, S.R.; Sheikh-El-Eslami, M.K. Risk Assessment of Virtual Power Plants Offering in Energy and Reserve Markets. *IEEE Trans. Power Syst. A Publ. Power Eng. Soc.* **2016**, *31*, 3572–3582. [[CrossRef](#)]
17. Da, T.; Zhang, D.; Ren, X.; Zhu, P.; Zhao, X.; Wu, N.; Liu, X. Non-Cooperative Game-based Coordination Control of Multiple Virtual Power Plants. In Proceedings of the 2021 IEEE Sustainable Power and Energy Conference (iSPEC), Nanjing, China, 25–27 November 2021.
18. Yin, S.; Ai, Q.; Li, Z.; Zhang, Y.; Lu, T. Energy management for aggregate prosumers in a virtual power plant: A robust Stackelberg game approach. *Int. J. Electr. Power Energy Syst.* **2020**, *117*, 105605. [[CrossRef](#)]
19. Zhou, Y.; Sun, G.; Huang, W.; Xu, Z.; Wei, Z.; Zhang, H.; Chu, Y. Strategic Bidding Model for Virtual Power Plant in Different Electricity Markets Considering Electric Vehicles and Demand Response. *Dianwang Jishu/Power Syst. Technol.* **2017**, *41*, 1759–1766.
20. Liu, S.; Ai, Q.; Zheng, J.; Wu, R. Bi-level Coordination Mechanism and Operation Strategy of Multi-time Scale Multiple Virtual Power Plants. *Zhongguo Dianji Gongcheng Xuebao/Proc. Chin. Soc. Electr. Eng.* **2018**, *38*, 753–761.
21. Yu, C.H.E.N.; Zhinong, W.E.I.; Zheng, X.U.; Wenjin, H.; Guoqiang, S.; Yizhou, Z. Optimal Scheduling Strategy of Multiple Virtual Power Plants Under Electricity Market Reform. *Dianli Xitong Zidonghua/Autom. Electr. Power Syst.* **2019**, *43*, 42–49.

22. Zahedmanesh, A.; Muttaqi, K.M.; Sutanto, D. A Consecutive Energy Management Approach for a VPP Comprising Commercial Loads and Electric Vehicle Parking Lots Integrated with Solar PV Units and Energy Storage Systems. In Proceedings of the 2019 1st Global Power, Energy and Communication Conference (GPECOM), Nevsehir, Turkey, 12–15 June 2019; IEEE: Piscataway, NJ, USA, 2019.
23. Goodarzi, M.; Li, Q. Evaluate the capacity of electricity-driven water facilities in small communities as virtual energy storage. *Appl. Energy* **2022**, *309*, 118349. [[CrossRef](#)]
24. Liu, Z.; Qin, L.; Yang, S.; Zhou, Y.; Wang, Q.; Zheng, J.; Liu, K. A comprehensive control strategy for photovoltaic virtual synchronous generator considering frequency regulation capability. *Energy Rep.* **2022**, *8*, 153–163. [[CrossRef](#)]
25. Wang, W.; Liu, H.; Ji, Y. Unified Modeling for Adjustable Space of Virtual Power Plant and Its Optimal Operation Strategy for Participating in Peak-shaving Market. *Dianli Xitong Zidonghua/Autom. Electr. Power Syst.* **2022**, *46*, 74–82.
26. Li, B.; Hao, Y.; Qi, B. Key Information Communication Technologies Supporting Virtual Power Plant Interaction. *Dianwang Jishu/Power Syst. Technol.* **2022**, *46*, 1761–1770.
27. Tong, L.; Zhao, S.; Jiang, H.; Zhou, J.; Xu, B. Multi-Scenario and Multi-Objective Collaborative Optimization of Distribution Network Considering Electric Vehicles and Mobile Energy Storage Systems. *IEEE Access* **2021**, *9*, 55690–55697. [[CrossRef](#)]
28. Yanfei, S.; Jiahui, W.; Geping, B.; Yue, C.; Yingjun, L.; Yuguang, N.; Pengcheng, Z. Multi-objective optimal dispatching of wind-photoelectric-thermal power-pumped storage virtual power plant. In Proceedings of the 2021 IEEE Sustainable Power and Energy Conference (iSPEC), Nanjing, China, 25–27 November 2021.
29. Hosseini, K.; Araghi, S.; Ahmadian, M.B.; Asadian, V. Multi-objective optimal scheduling of a micro-grid consisted of renewable energies using multi-objective Ant Lion Optimizer. In Proceedings of the 2017 Smart Grid Conference (SGC), Tehran, Iran, 20–21 December 2017.
30. Liu, N.; Zhao, J.; Wang, J. A Trading Model of PV Microgrid Cluster Based on Cooperative Game Theory. *Diangong Jishu Xuebao/Trans. China Electrotech. Soc.* **2018**, *33*, 1903–1910.
31. Muttaqi, K.M.; Sutanto, D. A Cooperative Energy Transaction Model for VPP Integrated Renewable Energy Hubs in Deregulated Electricity Markets. *IEEE Trans. Ind. Appl.* **2022**, *58*, 7776–7791.
32. Wang, X.; Zhang, H.; Zhang, S. Game Model of Electricity Market Involving Virtual Power Plant Composed of Wind Power and Electric Vehicles. *Dianli Xitong Zidonghua/Autom. Electr. Power Syst.* **2019**, *43*, 155–162.
33. Wang, X.; Shi, J.; Zhang, H.; Liu, Z.; Liu, D.; Li, H. Comprehensive evaluation method for energy efficiency of virtual power plants. In *IOP Conference Series: Earth and Environmental Science*; IOP Publishing: Bristol, UK, 2019.
34. Yufei, W.; Lei, H.; Chuangao, C. *An Improved NSGA-II for Coordinated Charging of Community Electric Vehicle Charging Station*; IEEE: Piscataway, NJ, USA, 2021.
35. Wang, S.; Zhao, D.; Yuan, J.; Li, H.; Gao, Y. Application of NSGA-II Algorithm for fault diagnosis in power system. *Electr. Power Syst. Res.* **2019**, *175*, 159–166. [[CrossRef](#)]
36. Sikorski, T.; Jasiński, M.; Ropuszyńska-Surma, E.; Węglarz, M.; Kaczorowska, D.; Kostyła, P.; Leonowicz, Z.; Lis, R.; Rezmer, J.; Rojewski, W.; et al. A Case Study on Distributed Energy Resources and Energy-Storage Systems in a Virtual Power Plant Concept: Economic Aspects. *Energies* **2019**, *12*, 4447. [[CrossRef](#)]
37. Wang, Y.; Liu, Z.; Cai, C.; Xue, L.; Ma, Y.; Shen, H.; Chen, X.; Liu, L. Research on the optimization method of integrated energy system operation with multi-subject game. *Energy* **2021**, *245*, 123305. [[CrossRef](#)]

Disclaimer/Publisher’s Note: The statements, opinions and data contained in all publications are solely those of the individual author(s) and contributor(s) and not of MDPI and/or the editor(s). MDPI and/or the editor(s) disclaim responsibility for any injury to people or property resulting from any ideas, methods, instructions or products referred to in the content.